COMPARISON OF THREE CHANGE DETECTION TECHNIQUES FOR MAPPING FIRE SCARS

Katherine Zdunic (1) **Graeme Behn** (1)

(1) Department of Conservation and Land Management
65 Brockway Road, Floreat Park, Western Australia
(08) 9333 6271, (08) 9333 6121
graemeb@calm.wa.gov.au

Abstract

Several classification techniques have been developed and used to detect and map burnt areas, ranging from the simple enhancements to the more complex, such as spectral unmixing and principal component analysis. In this project we used an historical sequence of rectified and calibrated Landsat Thematic Mapper (TM) imagery to produce a simulated pre-fire image. Near infrared and short wave infrared bands provide the best contrast between healthy vegetation and burned vegetation. Landsat TM bands 4 (near infrared) and 7 (short wave infrared) are combined in a band ratio transformation called the Normalized Burn Ratio (NBR = (B4 - B7)/(B4 + B7)). This transformation is computed for the simulated pre-fire image and then for each image date of the historical sequence. Fire occurrences for each date were mapped by subtracting the NBR of each date from the simulated pre-fire image. This method of mapping fire occurrences has been compared with two other multi-temporal fire detection techniques, and was found to produce the most reliable results of the three techniques.

Introduction

Remote sensing enables the historical mapping of fire scars over large areas. In many cases remotely sensed data is the only comprehensive data set available for inaccessible areas. Fires cause a temporary change in the landscape, therefore change detection methods may be used to map the occurrence of fires.

This study examines the performance of three change detection methods over a thirteen-date sequence of imagery in the Mount Barker Landsat TM scene, path 111, row 84. Indices improve the ability of one land type to be discriminated from another. An index for identifying fires in a single image is applied to each date and used as input into the change detection methods. The index utilised is the Normalised Burn Ratio (NBR) and it produces a single band image for each date, where the areas affected by fire have negative values. The change detection methods examined are fire effect, image differencing magnitude and simulated pre-fire image. The effectiveness of each technique is accessed visually with the aid of colour composite enhancements and geo-linked windows.

The most reliable change detection technique determined by this investigation, will be used to conduct fire history mapping throughout the south west of Western Australia. This information will increase knowledge of fire regimes and improve fire management practices.

Study Area

The study area is located in the south west of Western Australia in Landsat TM Mount Barker scene, path 111, row 84 as shown in figure one. The study area is separated into two zones for description and spectral signature analysis due to differences of rainfall, soils and vegetation. The whole study area however is applied at once in the analysis. The description of the regions focuses on the forested areas, the other major land use in the study area is agriculture. The production from these areas is dryland agriculture and plantations (Beeston *et. al.*, 2002).

The Stirlings region shown on figure one encompasses the Stirling Range National Park (SRNP) and the Porongurup National Park (PNP). The area experiences a typical Mediterranean climate, with the SPNP experiencing a greater range of temperatures due to being located further from the coast (Herford *et. al.*, 1999). The two parks although geographically close have different geology. The Stirling Range consists of altered sandstones and shales laid down at the coast of an ancient sea, a layer of clayey soil covers the mid slope level, with the best soils located on the valley floors (Herford *et. al.*, 1999). The hills of the Porongurup Range were granite islands 55 million years ago, the steep slopes contain rock screes and sandy deposits, the south west corner of the PNP includes a small area of deep sand (Herford *et. al.*, 1999). The SRNP consists of five

major plant communities including; thicket, mallee-heath, woodlands, wetlands and salt-lake communities (Keighery and Beard, 1994). The SRNP has a great diversity of flora making up over 20 percent of the known flora in Western Australia (Herford *et. al.*, 1999). The PNP is composed of three major plant communities; granite outcrops, surrounded by tall karri forest and jarrah, marri forest in the low woodland (Herford *et. al.*, 1999). The annual rainfall in the SRNP varies from 500-600mm with rainfall decreasing in the northern side of the park and greater precipitation on the peaks. The annual rainfall in the PNP is greater at 700mm (Herford *et. al.*, 1999).

The Western region as shown on figure one contains a large area of forest, which is made up of state forest, national parks and vacant crown land. Annual rainfall starts from 1400mm on the south west coast and decreases to the east and north to 700mm (Department of Agriculture, 2003). The climate of the region is a Mediterranean type. The forest on the south coast contains granite outcrops, areas of yellow duplex soils and a thin capping over rocks of laterite (Smith *et. al.*, 1990). Many of the plant species on the south west coastal forest are high rainfall species. Fourteen plant community types exist in this region, the types include various types of shrubland, heath, forest, dune and plain (Smith *et. al.*, 1990). The inland forest in the Western region also contains granite outcrops and yellow duplex soils are located in small amounts, grey gravelly sandy loams are more common. Further to the north clay soils and podsolic grey sands occur (Liddlelow and Ward, 1981). The vegetation formations present are open forest, low woodland, low open woodland, sedgelands/open heath and riverine (Liddlelow and Ward, 1981).

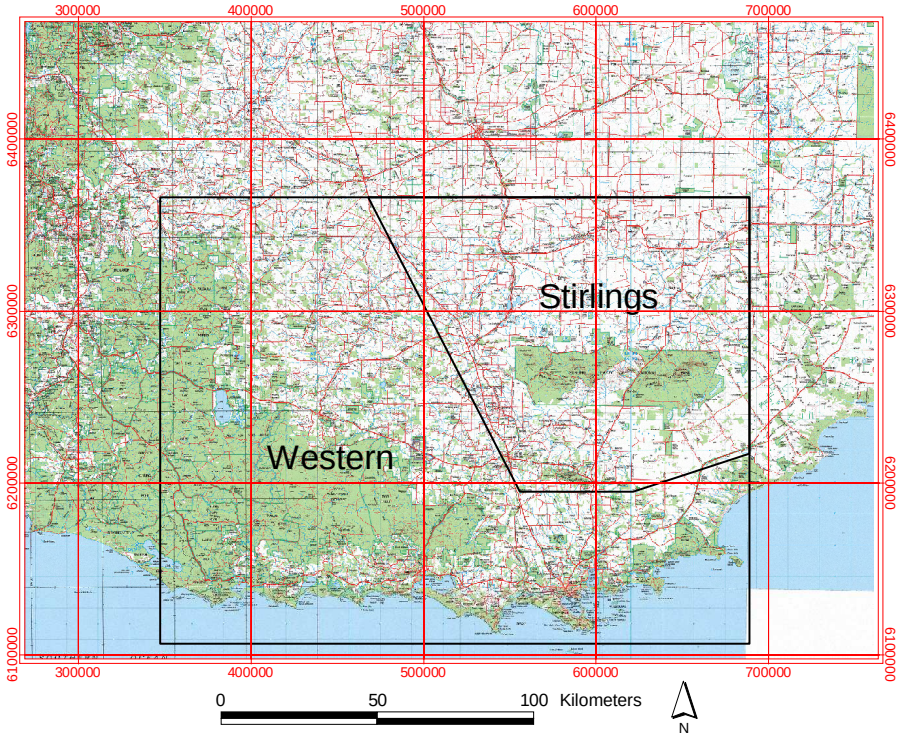

Figure 1: South west Western Australia, study area Mount Barker scene path 111, row 84.

Data set

The image sequence utilised consists of thirteen Landsat TM scenes, table one displays the image acquisition dates. Multi-temporal analysis requires that pixels represent the same position throughout time. Each scene was precisely registered to an accurate base mosaic of the area (Caccetta *et. al.*, 2000). The images were co-registered at 25 metre pixel, projection AMG, datum AGD66. Each image datum has been transformed to GDA94, thus the projection and datum used in this study is MGA zone 50, GDA94. Calibration is also a requirement for multi-temporal analysis, so that pixel values can be compared from different dates. The summer imagery is calibrated to a summer base which was cross calibrated using robust regression techniques to provide a consistent radiometric base (Caccetta *et. al.*, 2000), (Furby and Campbell, 2001). The spring imagery is similarly calibrated.

Mount Barker 111/84	Season
11 February 2002	Summer
28 March 2001	Summer
6 February 2000	Summer
11 February 1999	Summer
7 January 1998	Summer
20 March 1995	Autumn
28 January 1994	Summer
22 September 1993	Spring
24 February 1992	Summer
20 January 1991	Summer
14 September 1990	Spring
19 March 1989	Autumn
13 February 1988	Summer

Table 1: Landsat TM Mount Barker scenes, path 111, row 84, image acquisition dates.

Background

Fire Indices

Indices that identify fire in a single image are useful to use as base images in a temporal analysis of fire. An appropriate index will ensure the brightness values of fires in a single image will be higher or lower than other areas of the image. Most applications of an index however will identify fires and those areas with similar spectral signatures to fire. This is where temporal analysis can be introduced to remove those areas that are similar spectrally to fire.

Normalised difference vegetation index (NDVI) is a commonly used index that has been applied to fire mapping, (Garia-Haro *et. al.*, 2001), (Sunar and Özkan, 2001). Salvador *et. al.* (2000) applied NDVI to a sequence of Landsat MSS imagery to use in a semi-automatic method for detecting fire scars. The study found that NDVI was not as effective in areas of sparse vegetation and in areas where there has been significant

recovery of the vegetation after the fire instance. Thus due to the scrub-like vegetation of much of the study area this index would not be ideal.

Koutsias and Karteris (2000) examined the discriminator ability of the Landsat TM bands between fire and other land cover types. The study found that when differentiating between crops and fire scars band four and band seven provided the best discrimination, and band five and band seven provided the best discrimination between forest and fire scars. The study also examines the performance of indices and colour composites of identifying fires. The indices examined are the NDVI and a variation of NDVI using band seven and band four, in the place of band four and band three. It was found that this variation performed better than NDVI in identifying fire scars in a single image. Colour composites using band four, band seven and either band one or two provide the best red, green, blue enhancements of fire scars.

Key and Benson (2001) examine the effectiveness of the normalised burn ration (NBR), shown in equation (1) below. They examined the use of band 7, NDVI and NBR in conjunction with image differencing to identify fire severity. Image differencing is the subtraction of a pre-fire image from a post-fire image to identify areas of change. Areas of change will include fire scars and other changes such as forest clearing. Key and Benson found that NBR provided the best delineation between fire scars and unburned areas and NBR also had the largest dynamic range within the fire scars, which enabled fire severity to be mapped. NBR performed best when the images differenced were obtained in spring, as compared to late summer results.

$$\frac{TM\ band\ 4 - TM\ band\ 7}{TM\ band\ 4 + TM\ band\ 7} \qquad (1)$$

Application of the NBR to a single image produces a single band image that displays fire scars and areas with similar spectral signatures to fire, as dark regions. Figures two and three below show the spectral signatures of agricultural land, forest and fire scars of the two stratified regions in the Landsat TM scene used in the analysis, the values were extracted from the 1998 Mount Barker scene.

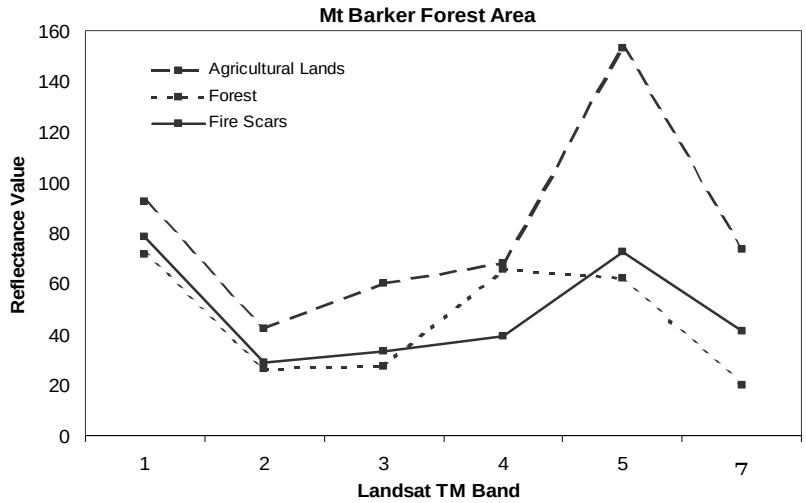

Figure 2: Average reflectance values for each Landsat TM band in the agricultural lands, forest and fire scars in the western region of the Mount Barker scene, extracted from the 1998 image.

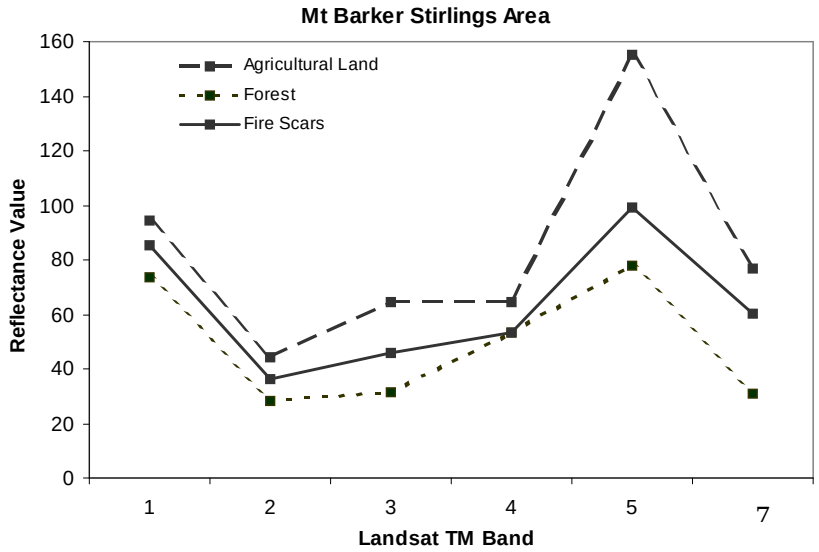

Figure 3: Average reflectance values for each Landsat TM band in the agricultural lands, forest and fire scars in the Stirlings region of the Mount Barker scene, extracted from the 1998 image.

Figures two and three show how the fire scars in the regions differ. In the Stirlings region the fire scars in bands four and seven are much brighter, and thus resemble agricultural lands more than in the western region where there is a larger gap in reflectance values. However when the NBR is calculated due to the similar differences in band reflectance values the NBR values for agricultural lands and fire scars in the Western region are very similar, this is illustrated in table 2. In the Stirlings region the agricultural areas NBR values are considerably more negative than the fire scars' NBR values. The ideal situation would be for the fire scars in both regions to have the highest negative values for ease of identification. In a single image this is not possible, but in a

temporal sequence the unchanging agricultural areas may be removed and the fire scars may be identified more readily.

Land Cover Type	Region	NBR value
Agricultural Lands	Western	-0.02797
Forest	Western	0.527763
Fire Scars	Western	-0.02555
Agricultural Lands	Stirlings	-0.10818
Forest	Stirlings	0.268164
Fire Scars	Stirlings	-0.04856

Table 2: NBR values for land types in the two regions identified in the Mount Barker 1998 Landsat TM scene.

Change detection for fire scars

Change detection is an effective tool in identifying fire scars. Other land use types having similar spectral signatures or derived index values to fire scars, affect single image assessments. If these similar areas do not change significantly over time then change detection may be used to remove them from the analysis, and focus on the changes caused by fire. Change detection requires that the sequence of imagery needs to be co-registered, the temporal resolution held constant and ideally captured by the same sensor (Jensen, 1996). Calibration to common reference values allows the comparison of images from different dates (Furby and Campbell, 2001). For fire detection it is best if the post-fire image is not captured more than a year after the fire incidence (White *et. al.*, 1996), therefore it is ideal if the image sequence is annual. Obtaining imagery from the same time of year will reduce seasonal affects on the analysis. The effectiveness of change detection is affected by changes in soil moisture conditions and vegetation phenological cycles (Jensen, 1996).

Fire Effect

The fire effect multi-temporal method of fire detection proposed by Garcia-Haro *et. al.* (2001) utilises a sequence of three images. One image refers to the pre-fire image, the second image is the first date after the fire incidence and the third image is the second date after the fire incidence. Garcia-Haro *et. al.* derived NDVI images to be used in the image sequence, this study uses NBR images in determining the fire effect measure, equation (2) displays the algorithm required to calculate the fire effect. R_1 is the first date subtracted from the second date and R_2 is the second date subtracted from the third date. P is an empirically determined negative factor, Garcia-Haro *et. al.* adopted a value of negative one for P and that value has also been used in this study.

$$Fire\ Effect = \frac{R_2 - R_1}{R_2 + R_1} R_1^P \qquad (2)$$

Values for fire effect will be higher and positive where there are large changes between the three input images, which corresponds with the temporary changes caused by fire. The fire effect is assessed for the second input image, which is the first image taken post-fire. Garcia-Haro *et. al.* compared the fire effect technique with two other methods, change vector analysis and multi-temporal principal components analysis. The authors found that all methods were effective in detecting forest fires, but the fire effect method yielded the most reliable results.

Image Differencing Magnitude

Image differencing is the subtraction of an image from another image of a different date to produce a change image. When using images produced by the calculation of the NBR the subtraction of the post-fire image from the pre-fire image yields an image where areas of change have higher values. Those changes associated with fire appear as large positive values. This method has been applied by Miller and Yool (2002) and Key and Benson (2001) to assess fire severity. The method applied in this study utilises the magnitude of the changes found in the change image, yielding an image where all the changes are positive, equation (3) displays the algorithm used. This method allows fires to be identified in two change images, one where the change is caused by the destruction of the fire, and in the later change image where the change is due to revegetation in the fire affected area.

$$Magnitude\ of\ \ Change = \sqrt{(\mathrm{Pr}\, eFire\ NBR - PostFire\ NBR)^2} \qquad (3)$$

Simulated Pre-fire Image

Fires cause a temporary change in the landscape, thus image differencing works well in highlighting those areas that have changed in one year to another. When identifying fires using image differencing the pre-fire image is ideally not affected by change, this however is difficult to achieve across an entire Landsat scene. Creating a simulated pre-fire image aims to construct a pre-fire image not affected by temporary changes. This is achieved by extracting the median value of a pixel from a large sequence of imagery. The median value is extracted, as throughout the sequence of imagery when the area of a pixel is burnt the reflectance value of the pixel will change between higher and lower values than the pre-fire pixel value. The sequence of imagery records when the area is charred, bare and at different levels of recovery until the area is restored to its pre-fire state.

To create a simulated pre-fire NBR image the median for each pixel in band four and in band seven needs to be found initially. Then using the pre-fire band four and band seven images the simulated pre-fire NBR may be derived. This is done to reflect the changes observed by the sensor. Then to identify fires in the post-fire image, the post-fire image

is subtracted from the simulated pre-fire image. Changes due to fire will appear as positive values.

Methodology

The analysis was carried out using ER Mapper 6.2. As a basis for all the change detection methods to be tested a single multi-band image containing the NBR calculated for each date was created. The NBR values where transformed from the possible range of values of -1, 1 to 0, 255 to enable the image to be saved in unsigned eight bit integer format. This process produced a thirteen band image. A water mask derived from the Landsat TM imagery is applied to the outputs of the three change detection methods due to areas of water being identified as change.

Fire Effect

Calculation of the fire effect requires three imagery dates and the resultant image can be used to identify fire scars that occurred after the first date and before the middle date. Therefore the resultant image is assigned to the middle date. In the sequence of the thirteen images the first and last dates will not have fire effect images assigned to them. To determine the fire effect firstly the R_1 and R_2 values are calculated utilising the multi-band NBR image, and stored in a two band image. The values for R_1 and R_2 were transformed from a possible range of –255, 255 to 0, 255. This two band image was then used to compute the fire effect. For display purposes the values of fire effect were stretched from a range of –0.01, 0.01 to 0, 255.

Image Differencing Magnitude

The method applied in this study finds the magnitude of changes between two dates. The changes found are ascribed to the more recent of the two dates, thus there is no change image produced for the oldest image in the sequence. The multi-band NBR image was used to compute the change images. The change images show areas of fire destruction and recovery as large positive values. In order to differentiate between destruction and recovery, previous change images need to be consulted to assign the earliest possible date to the fire occurrence.

Simulated Pre-fire Image

In order to calculate the median for each pixel in band four and band seven a program was written in the Java 2 language. As input the program required a multi-band image file containing each date in the sequence for a single band, in eight-bit integer, ER Mapper format. The output of the program is a single band image containing the median values for the input band in ER Mapper format. Once the median images for band four and band seven are produced they are saved to a two-band image file. This image is then added to the multi-band NBR image as another band and the NBR calculated to produce the simulated pre-fire image. To produce the change images each date is subtracted from the simulated pre-fire image. This method produces a change image for each date in the

sequence. The range of values in the change image is –255, 255 and changes due to fire appear as positive values, therefore the image is thresholded to the positive values in the image. This improves the differentiation of fire scars from the background.

Results

Comparing the results for a year in the image sequence and ranking the techniques assessed the results from the three change detection methods. The ranking was performed visually with two criteria, 1) the amount of fire scar identified and 2) the differentiation of the fire from the background. A ranking of one indicates the best performing method of the three in that particular year. A 7, 4, 2 RGB enhancement was also used in the assessment, figure four displays the four geo-linked windows used in the evaluation.

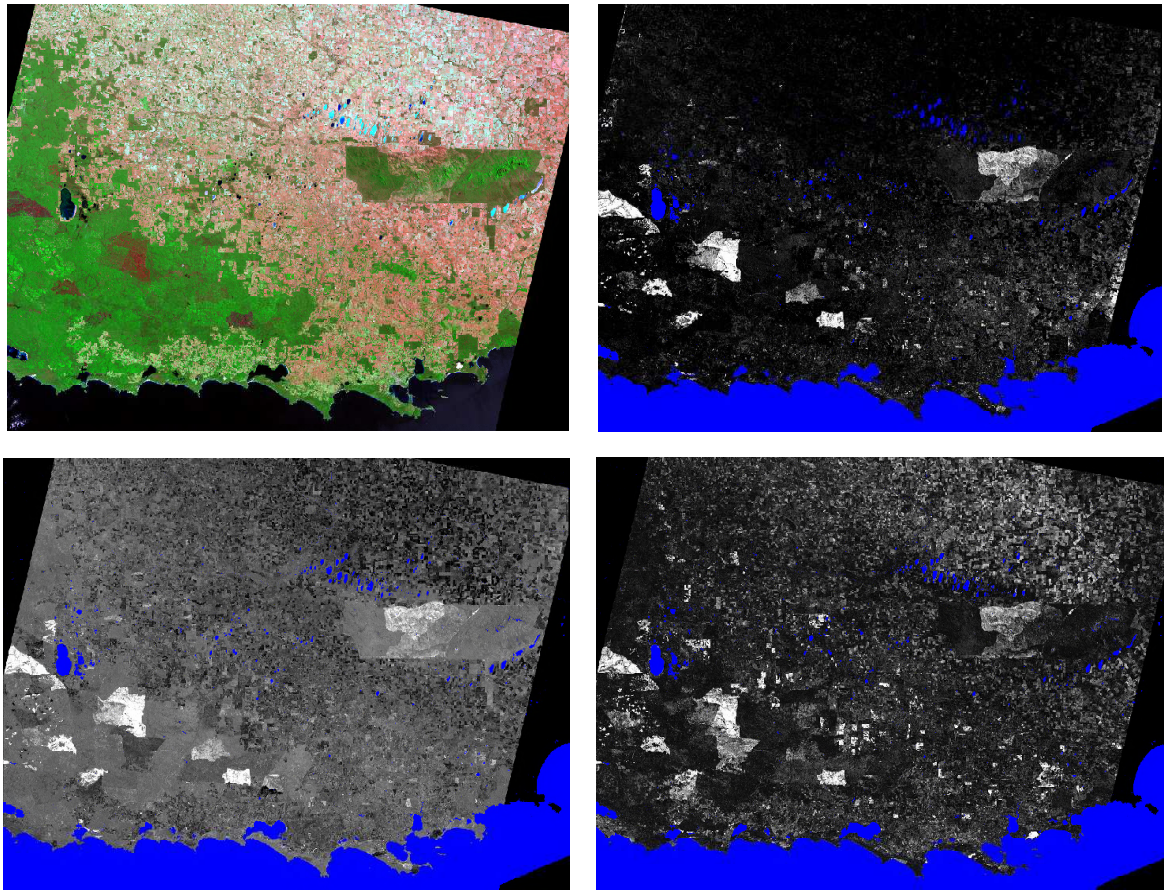

Figure 4: Ranking assessment images, 1998. Top left: bands 7, 4, 2 RGB enhancement, top right: simulated pre-fire change image, bottom left: fire effect change image, bottom right: image difference magnitude change image.

All the fire scars present in the images were examined and a ranking defined for the scene as a whole. Figure five illustrates a typical interrogation of the images. As can be seen in the enhancement one of the fires is barely perceptible and the other clearly visible. The value of the fire index in conjunction with change detection is shown in how the area of the barely perceptible fire in the enhancement is easily identified in the change images.

The clearly visible fire is defined quickly from all images but the other fire is not as well defined in the image differencing magnitude image. The fire effect and simulated pre-fire image identify the extents of that fire more completely, but the simulated pre-fire image defined the fire from the background more effectively. Therefore based on this area the ranking would be 1 – simulated pre-fire image, 2 – fire effect and 3 – image differencing magnitude.

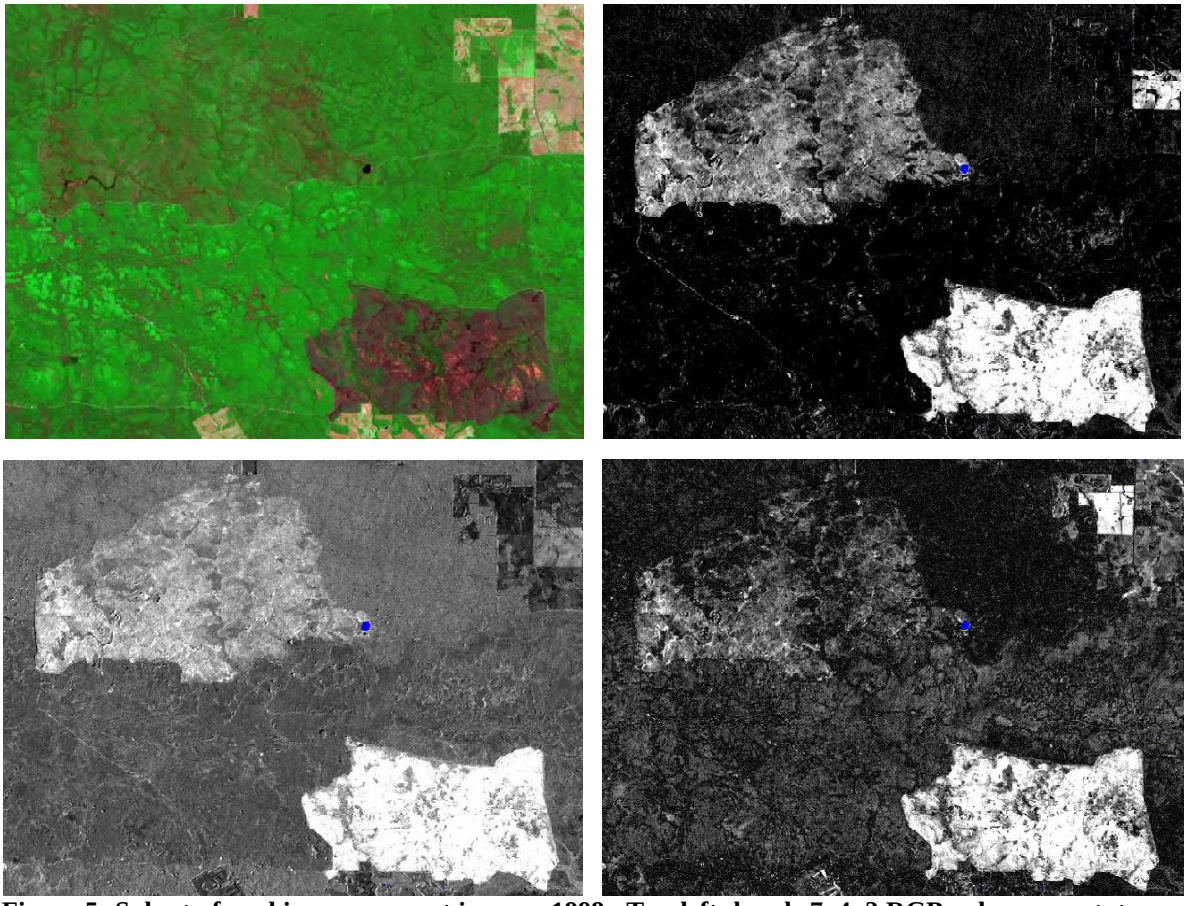

Figure 5: Subset of ranking assessment images, 1998. Top left: bands 7, 4, 2 RGB enhancement, top right: simulated pre-fire change image, bottom left: fire effect change image, bottom right: image difference magnitude change image.

Table 3 displays the rankings assigned for each year in the sequence and the average ranking obtained by each method. As can be seen the simulated pre-fire image performs the best followed by the fire effect method and lastly the image differencing magnitude technique. In 1989 the simulated pre-fire image did not perform as well as the other two techniques. This may be due to extensive cloud cover on the 1989 image, as the simulated pre-fire technique is dependant on the quality of the post fire image. The fire effect and image differencing magnitude methods were affected by the image quality of 1989 in the change detection image of 1990. This is due to 1989 being the pre-fire image in both techniques to determine the fire scars in 1990.

The possible causes for the failure of the simulated pre-fire image in 1992 are more difficult is ascertain. Upon examination of the imagery it appears that there is a flush of vegetation growth in the image. As the image was obtained in late summer the growth may have obscured the destruction caused by fires in the past year. Rainfall statistics for the Mount Barker area show a sharp increase in the amount of rain in February 1992. In February 1991 the total for the month was 2.6mm and in February 1992 the total was 39.0mm, most of which fell between the 1 and 13 February, the average for February is 24mm (Department of Agriculture, 2003).

Problems with a particular image will affect each change detection technique in different ways. The simulated pre-fire image method will be affected in the change detection image produced for the year of the image. The fire effect method effectiveness will be affected in the date after the problematic image. The image differencing magnitude technique is affected in the date after the problematic image, but it is not as severely affected as the fire effect method.

Year	Fire Effect	Image Differencing Magnitude	Simulated Pre-Fire Image
2002	-	2	1
2001	2	3	1
2000	3	2	1
1999	2	3	1
1998	2	3	1
1995	2	3	1
1994	2	3	1
1993	3	2	1
1992	1	2	3
1991	2	3	1
1990	3	2	1
1989	1	2	3
1988	-	-	1
Average Ranking	**2**	**3**	**1**

Table 3: Rankings assigned each fire detection method for each year in the sequence, a ranking of 1 indicates the best performance.

Discussion

All three techniques defined the fire scars acceptably when the fire had burnt the canopy, or the ground significantly. However fires which did not cause as much destruction or in which revegetation had occurred are harder to detect. The use of a geo-linked 7, 4, 2 RGB enhancement of the study area greatly improved the ability to identify fires from other changes detected by the three techniques. The analysis found that on average the simulated pre-fire image method of identifying fire scars performed the best compared to the other two change detection methods investigated. This could be due to this method providing a pre-fire image in which no pixel is affected by fire. The other two methods

can not provide this situation across an entire Landsat scene. The simulated pre-fire image technique however is strongly affected by the quality of the imagery.

The fire effect method identified fire scars capably, but does not differentiate the fire scar from the background as distinctly as the other two techniques. The effectiveness of the fire effect method suffers when the image quality of the pre-fire image is poor, or when the pre-fire or the first post-fire image is from a different season to the other two images. The image differencing magnitude technique identified the fire scars from the background suitably, but the extents of the fire scars were not identified as completely as the other two methods. The quality of the change detection images produced by the image differencing magnitude technique was most affected when the pre-fire image was a spring image and the post-fire image was a summer image. The image quality also affects the image differencing magnitude output, but not as significantly as the fire effect method.

The fire scars are clearly distinguished from the background in the forest areas. In the agricultural areas the fire scars are less easy to identify due to changes in the agricultural areas causing confusion. Stratification of the study area according to land use could improve the identification of fires in the agricultural areas. In the forest area of the Stirlings region the identification of the extent of fire scars is affected by the slow recovery of old fires. A new fire may burn into the area of a fire two or three years old and the extent of the old fire region burnt by the new fire can be difficult to delineate.

To create fire scar images from the change detection images the areas potentially affected by fire need to be extracted from the rest of the image. This may be achieved by generating vectors that roughly delineates the area of the fire scar detected and extracting those areas from the rest of the image. The shape and internal pattern of fire scars help to separate them from changes detected in the agricultural areas. The values in the fire scars are then reclassed to 0 and 1, with 0 representing areas not affected by fire and 1 representing areas that are affected by fire. This creates a binary image displaying the areas potentially affected by fire up to a year previous to the date of the image (White??). This time constraint was evident upon examination of the fire scars detected in 1998 and 1995, ground data for fires in 1996 were not evident in the fire scar map of 1998. Displaying several years of the fire scar history quickly shows the user the extent of fires in the study area.

The simulated pre-fire image technique of fire scar detection will be carried out on other Landsat TM scenes in the south west of Western Australia. The results from this analysis will be used to create fire history maps of the region. Interactive ArcView 3.2 projects will be created using this data and the projects will aid in understanding fire regimes and impacts in the south west of Western Australia.

References

Beeston, G.R., Hopkins, A.J.M. and Shepard, D.P. (2002) *Land-use and Vegetation in Western Australia: national land and water resources audit report*, Department of Agriculture, Perth, Western Australia, 107 pg.

Caccetta, P.A., Allan, A. and Watson, I. (2000) The Land Monitor Project, *Proceedings of the Tenth Australian Remote Sensing Conference*, 11 pg.

Deparment of Agriculture, Western Australia, *Climate Impacts and Weather Information*, URL: http://www.agric.wa.gov.au/climate/clig/climinfo/Climinfo.htm, accessed: 03/02/2003.

Furby, S.L. and Campbell, N.A. (2001) Calibrating Images from Different Dates to 'like-value' Digital Counts, *Remote Sensing of Environment*, Vol. 77, No. 2, pp. 186-196.

Garcia-Haro, F.J., Gilabert, M.A. and Melia, J. (2001) Monitoring Fire-affected Areas using Thematic Mapper Data, *International Journal of Remote Sensing*, Vol. 22, No. 4, pp. 533-549.

Herford, I., Gillen, K., Lloyd, M., Hine, C., McCaw, L., Keighery, G. and Allan, J. (1999) *Stirling Range National Park and Porongurup National Park Management Plan*, Department of Conservation and Land Management, Perth, Western Australia, 72 pg.

Jensen, J.R. (1996) Introductory Digital Image Processing: a Remote Sensing Perspective, Prentice-Hall, New Jersey, U.S.A., 316 pg.

Keighery, G. and Beard, J. (1994) Plants on the edge: vegetation and flora of the Stirling Range, Landscope, Vol. 10, No. 1, pp. 10-17.

Key, C. and Benson, N.C. (2001) *The Normalized Burn Ratio (NBR): a Landsat TM Radiometric Measure of Burn Severity*, URL: http://nrmsc.usgs.gov/research/ndbr.htm, accessed: 18/12/2002.

Koutsias, N. and Karteris, M. (2000) Burned Area Mapping using Logistic Regression Modeling of a Single Post-fire Landsat-5 Thematic Mapper Image, *International Journal of Remote Sensing*, Vol. 21, No. 4, pp. 673-687.

Liddelow, G.L. and Ward, C.G. (1981) *East of the Frankland: a biological survey*, Forests Department, Perth, Western Australia, 50 pg.

Miller, J.D. and Yool, S.R. (2002) Mapping Forest Post-Fire Canopy Consumption in Several Overstory Types using Multi-Temporal Landsat TM and ETM Data, *Remote Sensing of Environment*, Vol. 82, No. 2-3, pp. 481-496.

Salvador, R., Valeriano, J., Pons, X. and Diaz-Delgado, R. (2000) A Semi-Automatic Methodology to Detect Fire Scars in Shrubs and Evergreen Forests with Landsat MSS Time Series, *International Journal of Remote Sensing*, Vol. 21, No. 4, pp. 655-671.

Smith, V., Annear, R., Hanly, P., Metcalf, V., Sands, A. and Wardell-Johnson, G. (1990) *Walpole-Nornalup National Park: draft management plan*, Department of Conservation and Land Management, Perth, Western Australia, 211 pg.

Sunar, F. and Özkan, C. (2001) Forest Fire Analysis with Remote Sensing Data, *International Journal of Remote Sensing*, Vol. 22, No. 12, pp. 2265-2277.

White, J.D., Ryan, K.C., Key, C. and Running S.W. (1996) Remote Sensing of Fire Severity and Vegetation Recovery, *International Journal of Wildland Fire*, Vol. 6, No. 3, pp. 125-136.